

# Transcription Start Site Evolution in *Drosophila*

Bradley J. Main,<sup>\*1</sup> Andrew D. Smith,<sup>1</sup> Hyosik Jang,<sup>1</sup> and Sergey V. Nuzhdin<sup>1</sup>

<sup>1</sup>Section of Molecular and Computational Biology, Department of Biological Sciences, University of Southern California

\*Corresponding author: E-mail: bmain@usc.edu.

Associate editor: Stuart Newfeld

## Abstract

Transcription start site (TSS) evolution remains largely undescribed in *Drosophila*, likely due to limited annotations in non-melanogaster species. In this study, we introduce a concise new method that selectively sequences from the 5'-end of mRNA and used it to identify TSS in four *Drosophila* species, including *Drosophila melanogaster*, *D. simulans*, *D. sechellia*, and *D. pseudoobscura*. For verification, we compared our results in *D. melanogaster* with known annotations, published 5'-rapid amplification of cDNA ends data, and with RNAseq from the same mRNA pool. Then, we paired 2,849 *D. melanogaster* TSS with its closest equivalent TSS in each species (likely to be its true ortholog) using the available multiple sequence alignments. Most of the *D. melanogaster* TSSs were successfully paired with an ortholog in each species (83%, 86%, and 55% for *D. simulans*, *D. sechellia*, and *D. pseudoobscura*, respectively). On the basis of the number and distribution of reads mapped at each TSS, we also estimated promoter-specific expression (PSE) and TSS peak shape, respectively. Among paired TSS orthologs, the location and promoter activity were largely conserved. TSS location appears important as PSE, and TSS peak shape was more frequently divergent among TSS that had moved. Unpaired TSS were surprisingly common in *D. pseudoobscura*. An increased mutation rate upstream of TSS might explain this pattern. We found an enrichment of ribosomal protein genes among diverged TSS, suggesting that TSS evolution is not uniform across the genome.

**Key words:** promoter, transcription start site, gene expression, CAGE, TSS, *Drosophila*.

## Introduction

At a given gene, a functionally redundant promoter and associated transcription start site (TSS) may emerge ("birth") via random mutations, and similar to gene duplication events, one copy may experience relaxed selection (Ohno 1970). Ultimately, one copy "dies" or evolves a new function. Thus, a new TSS may arise or a TSS may move, or turnover, via this birth and death process (fig. 1). Conservation of TSS locations has mostly been explored between human and mouse, where TSS turnover (20%) (Frith et al. 2006) is reported to be less common than transcription factor binding site (TFBS) turnover (32–40%) (Dermitzakis and Clark 2002). However, regulatory divergence (including TSS movement) may be difficult to interpret at such evolutionary distances as mouse and human. Thus, comparisons among *Drosophila* species would be ideal, as multiple species genome alignments are available. For example, a recent study found that TFBS locations are highly conserved between *Drosophila* species in spite of extensive sequence turnover (Bradley et al. 2010). TSS turnover has been assessed in *Drosophila* but only for select genes (Sorourian 2010), including gene duplicates (Park and Makova 2009). We suspect that this is due to a lack of genome-wide TSS annotations in non-*Drosophila melanogaster* species. TSS annotations remain limited perhaps in part due to the lack of a clear canonical promoter motif (Ohler et al. 2002). Thus, the requirements for TSS initiation may be rather flexible, highlighting the importance of molecularly validated TSS in making quality annotations

and comparisons between species. Understanding TSS evolution is important because variants for TSS usage have been linked to important phenotypic differences (Wray 2003), including susceptibility to disease (Shin et al. 2000; Bonilla et al. 2006). Furthermore, promoter and TSS differences may account for important *cis*-regulatory differences (Wittkopp et al. 2004) between *Drosophila* species.

In this study, we developed a new method that identifies TSS and employed it to explore trends in TSS evolution in *Drosophila*. This concise method yields long (e.g., 76 bp), paired-end reads that are anchored to the 5'-end of mRNA. After mapping to each respective genome, we estimated and removed background noise using RNAseq reads (as a null model) generated from the same mRNA pool. Using this approach, we called TSS in four *Drosophila* species, including *D. melanogaster* (*mel*), *D. simulans* (*sim*), *D. sechellia* (*sec*), and *D. pseudoobscura* (*pse*). Then, we paired each *mel* TSS with its putative ortholog in each species (based on proximity) using the available multiple sequence alignment. From these results, we estimated overall and species-specific TSS differences, with respect to *mel*. For example, TSSs that are conserved in all but one species were considered species-specific TSS differences. Additionally, if a TSS variant was shared between *sim* and *sec* alone, we assumed the mutation event occurred before the split of these sister species. The relative abundance and distribution of coverage (TSS peak shape) at each TSS was highly reproducible between

© The Author 2013. Published by Oxford University Press on behalf of the Society for Molecular Biology and Evolution.

This is an Open Access article distributed under the terms of the Creative Commons Attribution Non-Commercial License (<http://creativecommons.org/licenses/by-nc/3.0/>), which permits non-commercial re-use, distribution, and reproduction in any medium, provided the original work is properly cited. For commercial re-use, please contact [journals.permissions@oup.com](mailto:journals.permissions@oup.com)

Open Access

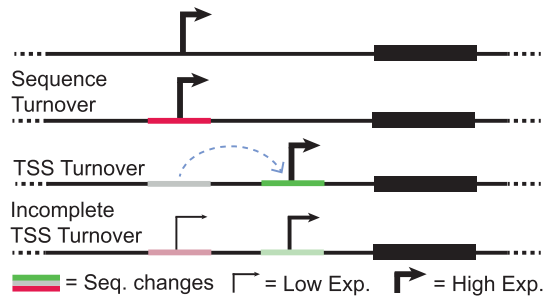


**Fig. 1.** Sequence turnover is indicated as color changes and TSS turnover as movement of TSS location. Note that expression and location are largely maintained during sequence turnover. TSS turnover is coincident with sequence changes and may be a gradual process.

biological and technical replicates, and expression estimates were comparable to RNAseq results generated from the same mRNA pool. Thus, we also estimated promoter-specific expression (PSE) and TSS peak shape for each species and compared conservation of promoter activity with the conservation of TSS location.

## New Approaches

### 5'-Anchored Reads

Several molecular techniques can be used to locate TSS including cap analysis for gene expression (CAGE) (Shiraki et al. 2003) and several updated versions (Ni et al. 2010; Plessy et al. 2010; Kanamori-Katayama et al. 2011), 5'-rapid amplification of cDNA ends (RACE) (Harvey and Darlison 1991), robust analysis of 5'-transcript ends (Gowda et al. 2007), and FLCDNA assays (Suzuki et al. 1997). The original CAGE protocol involves the concatenation of short 5'-sequence tags (14–20 bp), followed by traditional Sanger sequencing (Shiraki et al. 2003). More recently, CAGE and similar 5'-targeting methods have been adapted to high-throughput sequencing (Sandelin et al. 2007; Ni et al. 2010; Plessy et al. 2010; Kanamori-Katayama et al. 2011). One major difference between the available methods is the approach used to target 5'-ends of full length transcripts. For example, some methods rely on the removal of the 5'-cap structure with tobacco acid pyrophosphatase (TAP), others use the 5'-cap structure to perform template switching, and 5'-caps can also be biotinylated and isolated with streptavidin beads. We wanted a simple and straightforward approach without specific limitations, such as short reads (tags) (Harbers and Carninci 2005; Kodzius et al. 2006; Ni et al. 2010) and single-end reads (Kodzius et al. 2006), which hinder mapping, and added sampling bias from a required semisuppressive polymerase chain reaction (PCR) step (Plessy et al. 2010; Salimullah et al. 2011). Thus, we generated 5'-anchored reads using a concise TAP-based protocol that employs standard Illumina adapters and barcode indexes and is free of the aforementioned drawbacks. We extracted total RNA from whole body, adult female flies from each *Drosophila* species. We purified mRNA using oligo-dT Dynabeads (Invitrogen) and ligated an RNA adapter oligo to the 5'-end of each mRNA molecule. We chemically fragmented the

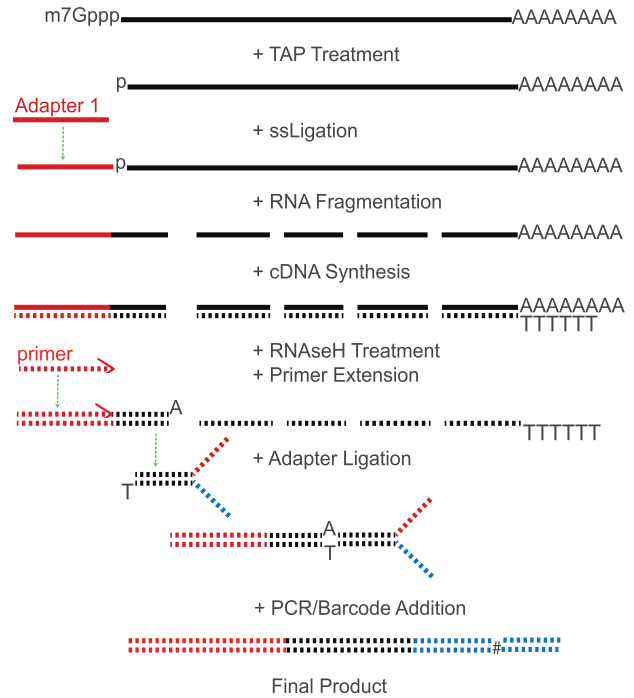


**Fig. 2.** Solid lines represent RNA and dashed lines indicate cDNA. Black lines are biological sequences, and red and blue represent Illumina adapters 1 and 2, respectively. Standard Illumina barcoding Indexes (see the # symbol) can be incorporated during PCR.

ligated mRNA using RNA fragmentation reagent (Ambion) and generated single-stranded cDNA with reverse transcriptase and random hexamers, followed by RNase H treatment. We added a primer complementary to the 5'-ligated adapter sequence and performed one primer extension step at 72 °C with Taq polymerase to yield double-stranded fragments of all 5'-ends (fig. 2). This primer has a 5'-amine group to prevent concatenation and subsequent ligation. Taq adds an A-overhang in a template-independent fashion (Clark 1988), thus we can bypass the typical blunt-end repair and cleanup step and immediately ligate standard Illumina adapters in a strand-specific orientation. Standard Illumina indexing barcodes were then added during PCR enrichment of each sample. We sequenced the 5'-enriched fragments on an Illumina Genome Analyzer II (see [supplementary file, Supplementary Material](#) online, for a detailed protocol).

One potential concern with using TAP treatment and RNA ligation is that RNA secondary structure might bias ligation. However, our results were highly reproducible, and expression estimates were similar with RNAseq results generated from the same mRNA pool (table 1). Also, we expect any bias in our sampling of TSS to be largely consistent between species, enabling us to compare TSS among species. Unlike typical 5'-RACE protocols, phosphatase treatment (e.g., using CIP) is optional in our protocol due to a required mRNA purification step, which leaves only trace amounts of uncapped product (e.g., rRNA). It is possible that fragmented or nonfull-length mRNA are present and could result in a false-positive TSS read. However, assuming break points are random, these signals would be removed as

background. As with any 5'-cap targeting method, results may include reads from transcripts that have broken and been recapped (ENCODE 2009).

Genome sequencing technology has advanced at an incredible rate making genome annotations a limiting factor in comparative genomics. This issue highlights the importance of methods similar to the one described here. Our method generates long, paired-end reads for improved mapping and the removal of PCR duplicates. This concise approach is amenable to projects with many samples and only requires 1–5 µg of total RNA, which is less than other methods that, like ours, do not rely on semisuppressive PCR (Shiraki et al. 2003; Kodzius et al. 2006; Ni et al. 2010). We believe this approach will be a valuable option for exploring TSS differences, improving genome annotations, and more generally, for gene expression studies where comparing PSE is important.

## Results and Discussion

### Analysis of 5'-Anchored Reads

We mapped the 76-bp paired-end reads to each respective reference genome of each species using the Burrows–Wheeler Aligner (BWA) (Li and Durbin 2009) (allowing 4% mismatches). We required that both reads in a pair mapped unambiguously, which allowed us to remove a substantial amount of PCR duplicates (table 2). The 5'-mapping position of the first read in each pair represents the TSS. We observed a prominent enrichment of reads mapped near known TSS in *mel*, but there was apparent background noise, likely due to residual RNAseq reads. Thus, we modeled the error in the

method using RNAseq reads generated from the same mRNA pool. We chose a threshold that removed 99% of positions identified from RNAseq (10 reads within 50 bp, see Materials and Methods). Next, we identified a single-representative TSS position centered in each cluster of TSS reads (TSS peak) to compare between species (see Materials and Methods). The majority of representative TSS positions (85%) and total reads mapped (84%) occurred within 200 bp of annotated 5'-transcript ends in *mel* (table 3). A previous CAGE study found a similar percent of reads that overlapped known TSS regions (86%) (Hoskins et al. 2011).

To determine whether the non-5'-end TSS peaks are likely new TSS or error, we explored these further. The non-5'-end TSS peaks included 301 that mapped to chromosome U and Uextra; sequences composed of unmapped heterochromatic regions of the genome that are arbitrarily concatenated together (Hoskins et al. 2007). Another 6% mapped within coding regions and 10% mapped to intergenic regions. Additionally, seven TSS peaks were identified at 5'-ends of protein-coding genes in the mitochondrial genome (e.g., Col-III and ND3). Here, we focused on PolIII transcripts, so mitochondrial TSSs were not analyzed further. We also avoided heterochromatic regions (i.e., TSS in chrU and chrUextra) of the genome because inherent challenges in sequencing, assembling, and localizing repeats in these regions may result in quality differences and limited alignments between species. Unexpected TSS locations are not unique to our TSS study (Frith et al. 2006; Hoskins et al. 2011) and may represent previously unannotated promoters, RNA breaks followed by recapping events (ENCODE 2009), or background noise from the method.

In summary, we compared 2,849 high confidence *mel* TSS with relative positions of TSS orthologs in *sim*, *sec*, and *pse*. It should be noted that this subset of *mel* genes is enriched for

**Table 1.** Method Reproducibility.

Comparison	$r^a$	P	$N^b$
5'-Anchored technical reps	0.91	<0.000001	759,628
5'-Anchored biological reps	0.87	<0.000001	2,471,760
RNAseq technical reps	0.86	<0.000001	132,600
RNAseq vs. 5'-anchored (FPKM)	0.60	<0.0001	NA

NOTE.—NA, not applicable.

<sup>a</sup>Pearson correlation coefficient.

<sup>b</sup>Sample size.

**Table 2.** Mapping Results.

Species	Method	Total RNA (µg)	Reads	Mapped	Percentage	Filtered <sup>a</sup>	Percentage
<i>mel</i>	CAGE	5	858,863	372,550	43	166,096	19 <sup>b</sup>
<i>mel</i>	CAGE	10	119,426	58,556	49	NA	NA
<i>sim</i>	CAGE	5	1,180,578	823,516	70	320,263	27
<i>sec</i>	CAGE	5	1,003,687	695,863	69	287,079	29
<i>mau</i> <sup>c</sup>	CAGE	5	627,904	286,214	46	NA	NA
<i>mau</i>	CAGE	5	1,201,745	488,569	41	NA	NA
<i>pse</i>	CAGE	5	1,161,039	822,188	71	323,942	28
<i>mel</i>	RNAseq	5	1,209,363	706,386	58	1,232,707	43 <sup>b</sup>
<i>mel</i>	RNAseq	10	1,664,075	1,004,598	60	NA	NA

NOTE.—NA, not applicable.

<sup>a</sup>Mapped reads after removing PCR duplicates.

<sup>b</sup>5 µg and 10 µg samples were pooled.

<sup>c</sup>*Drosophila mauritiana* was used for reproducibility estimates only.

**Table 3.** Accuracy of TSS Estimates.

Enrichment Category	Reads (%)	TSS (%)
5'-end (±200 bp)	83,237 (84%)	2,453 (85%)
CDS regions	5,673 (6%)	180 (6%)
Other	10,284 (10%)	240 (8%)

highly expressed genes, and extremely tissue-specific genes are under-represented (see [supplementary figs. S1 and S2, Supplementary Material](#) online). We attribute a portion of this bias to our conservative threshold for identifying TSS. However, as diverged TSSs were also enriched for highly expressed genes (see [supplementary fig. S1, Supplementary Material](#) online), our overall estimates of TSS conservation likely remain conservative.

### TSS Conservation between *Drosophila* Species

The birth of a new (alternative) TSS and TSS movement may contribute to regulatory variation, but the degree to which relative TSS locations are conserved among *Drosophila* is unknown. To assess TSS conservation in *Drosophila*, we paired each *mel* TSS with its ortholog in *sim*, *sec*, and *pse*. We accomplished this by converting the *mel* TSS position to an equivalent position in each species using the whole-genome pairwise alignment available from the UCSC genome browser and a LiftOver utility (see Materials and Methods). The most likely ortholog was then chosen based on proximity. Transcription initiates from a range of local positions at a given promoter, typically spanning less than 50 bp (Hoskins et al. 2011). Thus, we required that TSS orthologs be separated by more than 50 bp before we considered it as evidence for TSS movement. Intuitively, as the distance between putative orthologs increases, so does the likelihood that it was mispaired (e.g., with a promoter at a nearby gene). To limit this, we only paired TSS orthologs within 500 bp. Using this approach, we identified orthologous positions for nearly all the *mel* TSS in the sister species *sim* (96%) and *sec* (98%, [table 4](#)). We found much fewer orthologous positions in the more diverged *pse* (71%).

In total, 1,285 *mel* TSSs were paired with orthologs in all three other species, an additional 1,106 were paired with orthologs in at least two species, and an additional 296 *mel* TSSs were identified in only one species ([fig. 3](#)). We plotted the distribution of distances between all TSS orthologs for each species to elucidate any trends in TSS movement. This resulted in a sharp distribution of distances centered at 0 bp (relative to *mel*) between orthologous TSS for each species ([fig. 4](#)). Furthermore, only 4% of *mel* TSS between sister species and 9% between *pse* were separated by more than 50 bp. Thus, over 90% of the paired TSS locations were conserved in each *Drosophila* species, including the more distantly related *pse*. We expect these estimates of TSS conservation to be an overestimate because this trend excludes orthologs separated by more than 500 bp, movement less than 50 bp, TSS in unaligned regions, and TSS that were expressed below detection. For example, 13–16%

of *mel* TSS locations had identifiable orthologous positions but lacked an orthologous TSS within 500 bp in a given species. Unaligned regions prevented the identification of another 4%, 2%, and 29% of *mel* TSS regions in *sim*, *sec*, and *pse*, respectively ([table 4](#)). Many of these cases likely involve substantial evolutionary events. For example, we observed a *sec*-specific deletion at a promoter ([fig. 5](#)). Improved multiple species alignments, exhaustive sequencing coverage, combinations of sequencing approaches, and tests between more intermediate species (e.g., *D. yakuba* and *D. erecta*) and even comparisons within species may further help track highly diverged orthologous sequences and TSS movement between *Drosophila* species.

We hypothesized that TSS divergence accounts for important *cis*-regulatory differences between species. Thus, we identified cases of species-specific TSS movement. We assumed that cases of TSS divergence in both *sim* and *sec* exist due to a mutation before their speciation event ([fig. 6](#)). Similarly, if a *mel* TSS was diverged in all species, based on parsimony, we considered it as *mel*-specific TSS movement. Similar to our overall results, we report cases of species-specific TSS differences in three distinct categories of promoter divergence: paired but separated by more than 50 bp, mapped but unpaired, and unmapped. As expected, we observed similar species-specific differences for *sim* and *sec*, due to their equal divergence time from *mel* ([fig. 6](#)). However, unmapped TSSs were more common in *sim* (65 vs. 18), likely due to differences in genome quality between species. The *pse*-specific TSS differences were highest in all categories as expected due to its higher divergence time. The *mel* TSS positions that did not align between species likely indicate considerable sequence divergence at these regions. This may occur from movement of the entire TSS followed by

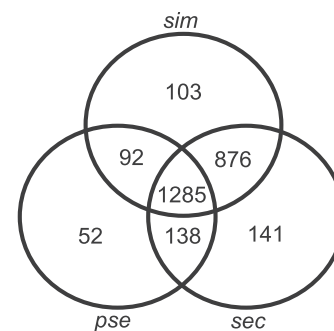


**Fig. 3.** The number of overlapping *mel* orthologs found in each species is shown. For example, 1,285 *mel* TSS had an identified ortholog in each species, and another 103 *mel* orthologs were only found in *sim*.

**Table 4.** Mapping Percentages of *mel* TSS to each Species.

Species	Mapped (%)	Unpaired <sup>a</sup> (%)	Paired (%)	<50 bp (%) <sup>b</sup>	>50 bp (%) <sup>b</sup>
<i>sim</i>	2,730 (96%)	374 (13%)	2,356 (86%)	2,242 (95%)	114 (5%)
<i>sec</i>	2,799 (98%)	359 (13%)	2,440 (87%)	2,332 (96%)	108 (4%)
<i>pse</i>	2,036 (71%)	469 (16%)	1,567 (77%)	1,385 (88%)	182 (12%)

<sup>a</sup>Unpaired *mel* TSS do not include unmapped.

<sup>b</sup>Percent out of all paired.

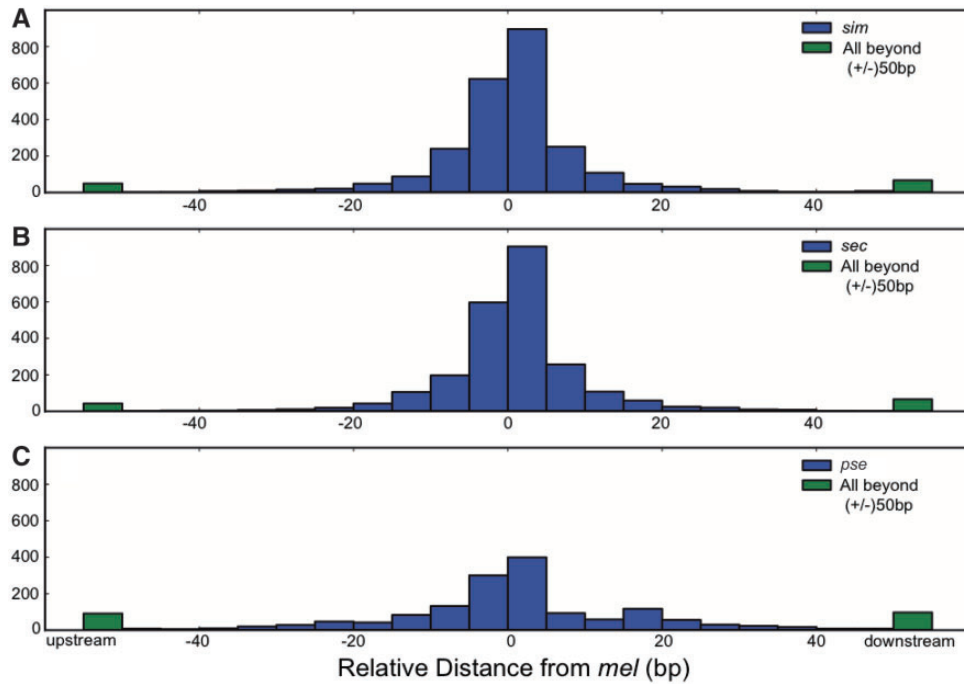


**FIG. 4.** These histograms show that *mel* TSS locations are largely conserved in *sim* (A), *sec* (B), and *pse* (C). Distances were calculated with respect to *mel* and the coding region. Thus, positive numbers are downstream from *mel* and negative values are upstream from *mel*.

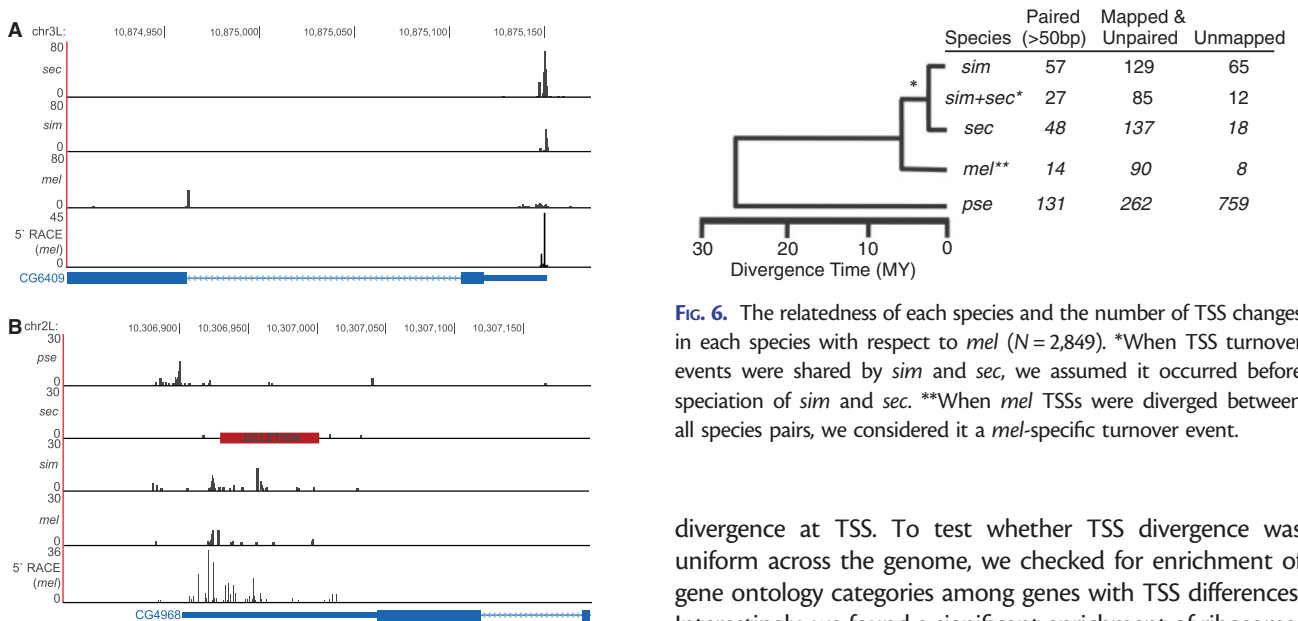


**FIG. 5.** Detailed examples of TSS variation between species. (A) There is a *mel*-specific, downstream TSS in CG6409, associated with the broadening of the upstream TSS. This may be an intermediate TSS turnover event. *pse* is not aligned in this region. (B) A *sec*-specific deletion (red square) at the TSS associated with nearly a complete loss of activity in *sec*. Also, predominant *pse* activity appears to have shifted 20 bp upstream.

**FIG. 6.** The relatedness of each species and the number of TSS changes in each species with respect to *mel* ( $N = 2,849$ ). \*When TSS turnover events were shared by *sim* and *sec*, we assumed it occurred before speciation of *sim* and *sec*. \*\*When *mel* TSSs were diverged between all species pairs, we considered it a *mel*-specific turnover event.

degeneration of the now nonfunctional promoter element or a duplication event that prevents unambiguous alignment. We believe the relative proportion of *mel* TSS that do not map between species is an informative estimate of sequence

divergence at TSS. To test whether TSS divergence was uniform across the genome, we checked for enrichment of gene ontology categories among genes with TSS differences. Interestingly, we found a significant enrichment of ribosomal protein genes for each species ( $P = 1.4e-16$ ). Perhaps, TSS movement and sequence turnover have hindered the discovery of functional regulatory elements for these genes (Hu and Li 2007). Overall, we observed highly conserved TSS locations between each species, which is in contrast to estimates among mammals (Frith et al. 2006).

Considering that promoters are essential regulatory elements, we were surprised that 29% of *mel* TSS positions did not map to *pse*. Positive selection on distinct elements or an increased mutation rate in TSS proximal DNA might explain this elevated sequence divergence. To test this, we explored patterns of local sequence conservation flanking the TSS.

Interestingly, there is a prominent increase in sequence divergence upstream of the TSS among insects (fig. 7). If positive selection has occurred between species, we might expect increased divergence between species and reduced sequence variation within species. Thus, we examined mutation frequencies within a population of *mel*. We observed a trend of increased variation (elevated frequency of segregating mutations) upstream of the TSS that coincided with reduced sequence conservation between species (fig. 7D). This suggests that an increased mutation rate upstream of TSS might be the source.

### Conservation of Promoter-Specific Expression (PSE) and TSS Peak Shape

Expression profiles from our 5'-anchored reads were highly reproducible between technical and biological replicates (Pearson correlation,  $r = 0.91$ ,  $P < 0.0001$  and  $r = 0.87$ ,  $P < 0.0001$ , respectively; table 1), and expression estimates (FPKM) were highly correlated with standard RNAseq derived from the same RNA pool ( $r = 0.60$ ,  $P < 0.0001$ ). Thus, we did not detect substantial bias from the method. We estimated PSE from the total number of reads that map within 50 bp of

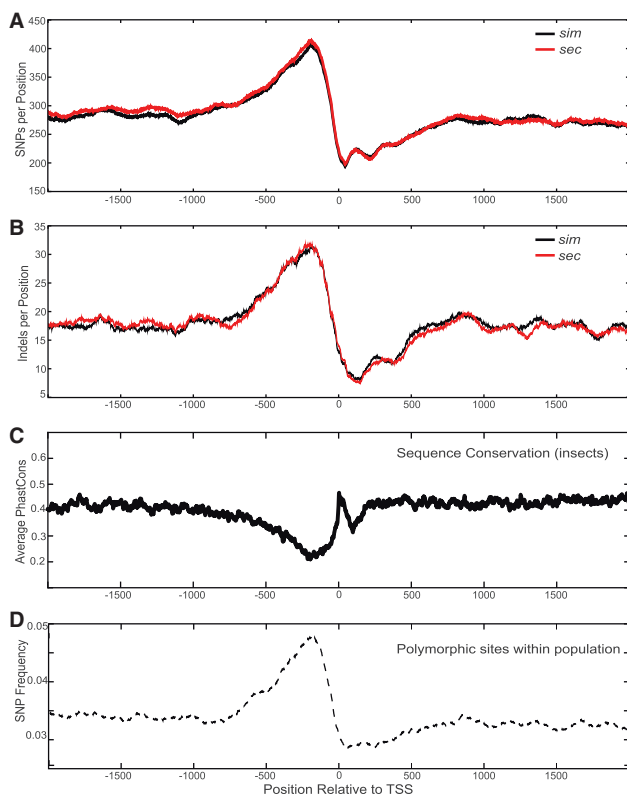


**Fig. 7.** We examined patterns of sequence conservation within 2 kb of *mel* TSS ( $N = 2,849$ ). (A) The trend of SNPs around all *mel* TSS in *sim* (black) and *sec* (red). This plot shows the averages of a 100 bp sliding window. (B) Similar to (A), but with indels. (C) Plotted are the average sequence conservation (PhastCons 15 insect species) scores around TSS. Note that there is a dip in conservation corresponding with the spike in mutations between *mel* and *sim*. (D) We examined *mel* population data and plotted the frequency of segregating sites around TSS. This spike in sequence diversity upstream of TSS indicates that there is likely an increased mutation rate upstream of TSS.

each representative TSS position. We normalized each PSE estimate by dividing by the total number of reads mapped in each sample. To illustrate the type of data we generated and the value of estimating PSE, we describe species-specific usage of two alternative promoters of alcohol dehydrogenase (ADH), a highly studied gene important in ethanol preference and tolerance in fermenting food (Malherbe et al. 2005; Ogueta et al. 2010). These alternative promoters are known to be tissue specific and temporally regulated (Posakony et al. 1985). The proximal TSS is favored in *mel*, *sim*, and *sec* to varying degrees, but *pse* exclusively uses the distal TSS in adult females (fig. 8). Interspecific differences in expression from these alternative promoters has been observed previously, but an adaptive link has not been reported (Papaceit et al. 2004).

Highly significant correlations in PSE were found between *Drosophila* species (Pearson correlation,  $r = 0.63$ ,  $P < 0.0001$ ;  $r = 0.66$ ,  $P < 0.0001$ ; and  $r = 0.54$ ,  $P < 0.0001$  for *sim*, *sec*, and *pse*, respectively; table 5). TSS movement may significantly alter the suite of regulatory elements associated with each promoter. Thus, we hypothesized that PSE differences will increase between TSS that have moved. To test this, we compared correlations in PSE between TSS with conserved locations and TSS that have moved beyond 50 bp. For conserved TSS, correlations in PSE increased relative to the overall estimates ( $r = 0.65$ ,  $P < 0.0001$ ;  $r = 0.68$ ,  $P < 0.0001$ ; and  $r = 0.57$ ,  $P < 0.0001$  for *sim*, *sec*, and *pse*, respectively; table 5). Interestingly, the minority of paired TSS orthologs that have moved beyond 50 bp have more differences in expression ( $r = 0.17$ ,  $P = 0.07$ ;  $r = 0.26$ ,  $P = 0.006$ ; table 5). This result highlights the importance of the relative position of TSS on maintaining gene expression levels.

Contrary to many “textbook” descriptions of transcription initiation in eukaryotes, transcripts start from a range of local positions at a given promoter. This results in a frequency distribution of initiation events that varies between promoters from “broad” to “sharp” (Ohler et al. 2002; Carninci et al. 2006; Nickel and Seedorf 2008; Rach et al. 2009). These “broad” and “sharp” structures are reproducible and largely conserved between mouse and human (Carninci et al. 2006) and between life stages of *Drosophila* (Hoskins et al. 2011). Comparisons between *Drosophila* species have only been made on select genes (Park and Makova 2009; Sorourian 2010). In this study, we roughly quantify the structure at each promoter using an entropy-based model (see Materials and Methods) and compare estimates between orthologs. Using this approach, we report that TSS initiation distributions are highly correlated between all species (Pearson correlation,  $r = 0.75$ ,  $P < 0.0001$ ;  $r = 0.76$ ,  $P < 0.0001$ ; and  $r = 0.66$ ,  $P < 0.0001$  for *sim*, *sec*, and *pse*, respectively; table 6). Roughly, sharp peaks remain as sharp peaks between species (and vice versa). Similar to PSE, correlations between TSS distributions increase when TSS location is conserved ( $r = 0.77$ ,  $P < 0.0001$ ,  $r = 0.79$ ,  $P < 0.0001$ ,  $r = 0.70$ ,  $P < 0.0001$  for *sim*, *sec*, and *pse* respectively) and decrease when TSSs are separated by more than 50 bp ( $r = 0.06$ ,  $P = 0.56$ ,  $r = 0.30$ ,  $P = 0.002$ ,  $r = 0.11$ ,  $P = 0.15$

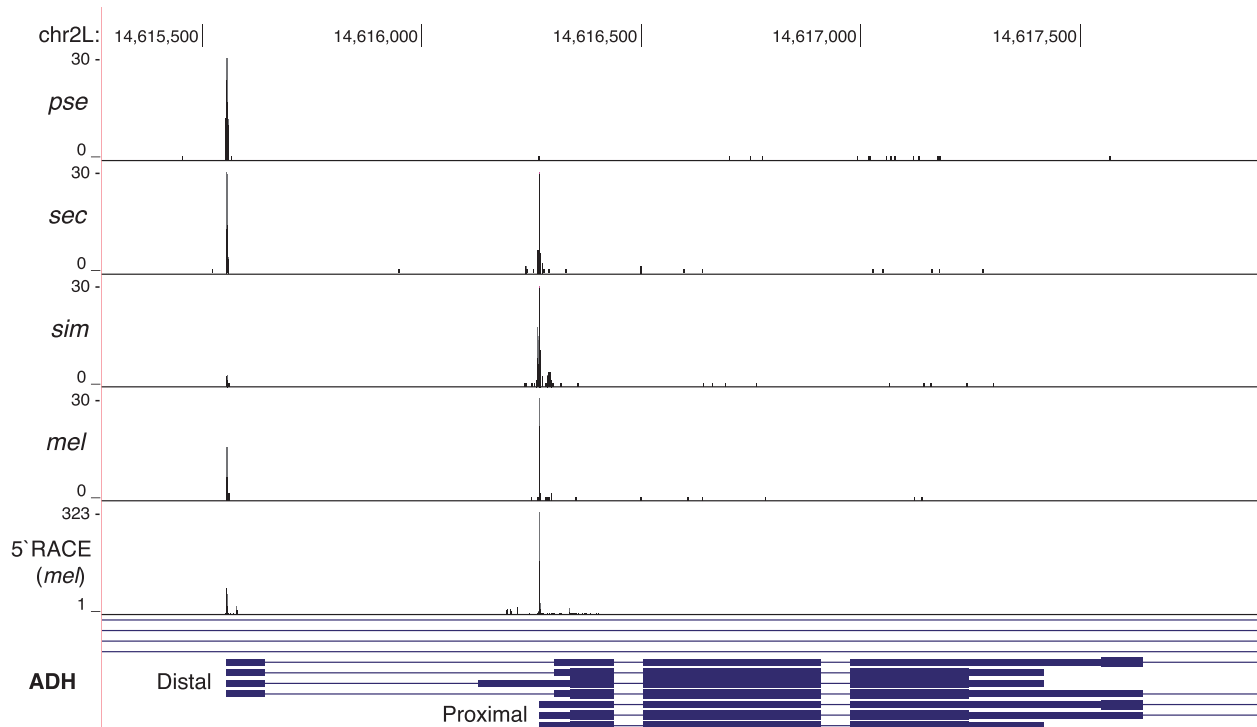


**FIG. 8.** In the ADH gene, we observe significant differences in PSE between species. For example, *mel* has biased expression of the downstream promoter, such as *sec*. However, *pse* is restricted to the upstream alternative promoter and *sim* is restricted to the downstream promoter.

**Table 5.** Conservation of Promoter-Specific Expression between Species.

Species	$r$ (All) <sup>a</sup>	N <sup>b</sup>	P	$r$ (TSS < 50 bp) <sup>c</sup>	N	P	$r$ (TSS > 50 bp)	N	P
<i>sim</i>	0.63	2,381	9.1e-261	0.65	2,266	1.9e-268	0.17	115	0.07
<i>sec</i>	0.66	2,448	7.9e-301	0.68	2,340	4.3e-315	0.26	108	0.006
<i>pse</i>	0.54	1,585	8.9e-120	0.57	1,400	5.4e-119	0.22	185	0.002

<sup>a</sup> $r$  = Pearson correlation coefficient.

<sup>b</sup>N = Sample size.

<sup>c</sup> $r$  < 50 bp are correlations limited to orthologs within 50 bp.

**Table 6.** Conservation of TSS Peak Shape between Species.

Species	$r$ (All)	N	P	$r$ (< 50 bp)	N	P	$r$ (> 50 bp)	N	P
<i>sim</i>	0.75	2,381	0.0	0.77	2,266	0.0	0.06	115	0.54
<i>sec</i>	0.76	2,448	0.0	0.79	2,340	0.0	0.30	108	0.002
<i>pse</i>	0.66	1,585	6.1e-202	0.70	1,400	4.2e-209	0.11	185	0.15

for *sim*, *sec*, and *pse* respectively; table 6). Thus, the relative location of TSS is important for maintaining several aspects of promoter activity. A previous study highlighted a species-specific change in TSS peak shape (Sorourian 2010). In support of this, we observed several cases of divergence in TSS peak shape from sharp to broad (with respect to the inferred ancestral state) coinciding with the birth of a new TSS (fig 5A).

## Materials and Methods

### Fly Strains

We used the following *Drosophila* strains in this study: *Drosophila melanogaster*: DGRP line hybrid of 303 and 313.

Bloomington stock: 25176 and 25180, respectively. *Drosophila simulans*: *st e* line; UCSD stock: 14021 0251.034. *Drosophila pseudoobscura*: UCSD stock: 14011 0121.32. *Drosophila sechellia*: Robertson Line 1. *Drosophila mauritiana*: w140 (used in reproducibility estimates).

### CAGE Library Preparation

We collected 20 virgin females from each *Drosophila* species and snap-froze them in liquid nitrogen in the morning as 3–5-day-old adults before storing them at  $-80^{\circ}\text{C}$  until further processing. We extracted total RNA using the ZymoResearch duet Kit. We prepared CAGE libraries for each of the five *Drosophila* species using 5  $\mu\text{g}$  of total RNA (fig. 2). First,

we used Dynabeads to isolate mRNA by polyA selection. Then, we treated the mRNA with TAP, which removes a pyrophosphate from the 5'-cap structure and exposes a 5'-phosphate to ligation with an RNA oligo (containing a Solexa adapter sequence). Next, we used RNA fragmentation reagent (Ambion) to randomly fragment the adapter-ligated mRNA before converting to single-stranded cDNA. We enriched for 5'-fragments by adding a primer that is homologous to the ligated RNA adapter oligo and performing one round of polymerase extension using Taq DNA Polymerase (*Thermus aquaticus*). Taq was specifically chosen because it adds an A at the end of each fragment in a template-independent fashion (Clark et al. 2006). Thus, after Taq extension (hence the name: Taq-ex CAGE), all 5'-fragments are double-stranded with an A-overhang on one end. From here, the standard RNAseq protocol is followed including adapter ligation, size selection, and index addition with PCR enrichment. A detailed protocol is available in [supplementary materials, Supplementary Material](#) online.

### Mapping CAGE Reads

Sequencing on an Illumina GAll with 76-bp reads resulted in over 1 million paired-end reads per species library (table 2). For a given species, the raw paired-end reads were mapped to their own genome using BWA version 0.5.9-r16. We mapped *D. simulans* reads to droSim1, *D. sechellia* reads to droSec1, *D. pseudoobscura* reads to dp4, and *D. mauritiana* reads to a DroMau draft genome (Nolte et al. 2013) (used for reproducibility estimates only). We allowed 4% mismatches and only accepted uniquely mapping reads. Next, PCR duplicates were removed using picards Mark Duplicate Reads (version 1.56.0).

### TSS Peak Calling

TSSs were identified from the paired-end CAGE data from the 5'-mapping position of the first read in each pair. Active promoters are represented as a frequency distribution of initiation events along the genome. We filtered for promoter regions with a minimum of 10 reads mapped within 50 bp, similar to Hoskins et al. (2011). At each promoter, we identified the average position used within the local frequency distribution of initiation events. Then, we chose the highest expressed TSS within 500 bp in *D. melanogaster* for comparisons between species. Thus, alternative TSSs were compared only if they were separated by 500 bp or more.

### TSS Peak Shape Quantification

To quantify peak shape, we calculated an entropy-based score within a 65-bp window centered on each TSS, similar to Hoskins et al. (2011). For some positions within the window, there may be zero reads mapped resulting in a probability of 0, underestimating of the true probability. The approach used by Hoskins et al. (2011) excluded these positions from the analysis, which effectively results in variable window sizes for each TSS distribution. When the window sizes are different, entropy estimates will be biased. Thus, we

incorporated Laplace's rule to account for cases of zero hits before calculating entropy. This approach adds a uniform probability (one mapped TSS read) across the entire window before estimating entropy. Here is the equation for our entropy-based score ( $E$ ) estimated at each TSS:  $E = -\sum_{i=0}^{65} p_i \log_2 p_i$ . It should be noted that entropy estimates for bimodal peaks or other higher order peak shapes may be overestimated using this method.

### Connecting Orthologs

We created an interval file with each TSS peak position found in *D. melanogaster* and converted these chromosomal positions to coordinates in the *D. simulans* (droSim1), *D. sechellia* (droSec1), and *D. pseudoobscura* (dp4) genomes using a LiftOver utility (Convert Genome Coordinates [Version 1.0.3]) available on the web-based galaxy platform (Giardine et al. 2005; Blankenberg et al. 2010; Goecks et al. 2010). Starting with the *D. melanogaster* TSS position converted to *D. simulans* (for example), we paired putative TSS orthologs based on proximity in *D. simulans* within 500 bp.

### Supplementary Material

Supplementary file and figures S1 and S2 are available at *Molecular Biology and Evolution* online (<http://www.mbe.oxfordjournals.org/>).

### Acknowledgments

The authors thank J.P. Masly for donating fly stocks and Christian Schlotterer for sharing genomic data. They also thank Johanna Main and Joe Dunham for discussions about the article and the method, respectively. This work was supported by the National Institutes of Health (grant numbers RO1 MH091561 and P50 HG002790 to S.V.N.).

### References

- Blankenberg D, Von Kuster G, Coraor N, Ananda G, Lazarus R, Mangan M, Nekrutenko A, Taylor J. 2010. Galaxy: a web-based genome analysis tool for experimentalists. *Curr Protoc Mol Biol*. Chapter 19:Unit 19.10.1–21.
- Bonilla C, Panguluri RK, Taliaferro-Smith L, et al. (22 co-authors). 2006. Agouti-related protein promoter variant associated with leanness and decreased risk for diabetes in West Africans. *Int J Obes (Lond)*. 30:715–721.
- Bradley RK, Li Xy, Trapnell C, Davidson S, Pachter L, Chu HC, Tonkin LA, Biggin MD, Eisen MB. 2010. Binding site turnover produces pervasive quantitative changes in transcription factor binding between closely related *Drosophila* species. *PLoS Biol*. 8:e1000343.
- Carninci P, Sandelin A, Lenhard B, et al. (41 co-authors). 2006. Genome-wide analysis of mammalian promoter architecture and evolution. *Nat Genet*. 38:626–635.
- Clark JM. 1988. Novel non-templated nucleotide addition reactions catalyzed by procaryotic and eucaryotic DNA polymerases. *Nucleic Acids Res*. 16:9677–9686.
- Clark RM, Wagler TN, Quijada P, Doebley J. 2006. A distant upstream enhancer at the maize domestication gene *tb1* has pleiotropic effects on plant and inflorescent architecture. *Nat Genet*. 38:594–597.
- Dermitzakis ET, Clark AG. 2002. Evolution of transcription factor binding sites in Mammalian gene regulatory regions: conservation and turnover. *Mol Biol Evol*. 19:1114–1121.



- ENCODE. 2009. Post-transcriptional processing generates a diversity of 5'-modified long and short RNAs. *Nature* 457:1028–1032.
- Frith MC, Ponjavic J, Fredman D, Kai C, Kawai J, Carninci P, Hayashizaki Y, Sandelin A. 2006. Evolutionary turnover of mammalian transcription start sites. *Genome Res.* 16:713–722.
- Giardine B, Riemer C, Hardison R, et al. (13 co-authors). 2005. Galaxy: a platform for interactive large-scale genome analysis. *Genome Res.* 15: 1451–1455.
- Goecks J, Nekrutenko A, Taylor J, Galaxy Team. 2010. Galaxy: a comprehensive approach for supporting accessible, reproducible, and transparent computational research in the life sciences. *Genome Biol.* 11:R86.
- Gowda M, Li H, Wang G. 2007. Robust analysis of 5'-transcript ends: a high-throughput protocol for characterization of sequence diversity of transcription start sites. *Nat Protoc.* 2:1622–1632.
- Harbers M, Carninci P. 2005. Tag-based approaches for transcriptome research and genome annotation. *Nat Methods.* 2:495–502.
- Harvey RJ, Darlison MG. 1991. Random-primed cDNA synthesis facilitates the isolation of multiple 5'-cDNA ends by RACE. *Nucleic Acids Res.* 19:4002.
- Hoskins RA, Carlson JW, Kennedy C, et al. (14 co-authors). 2007. Sequence finishing and mapping of *Drosophila melanogaster* heterochromatin. *Science* 316:1625–1628.
- Hoskins RA, Landolin JM, Brown JB, et al. (19 co-authors). 2011. Genome-wide analysis of promoter architecture in *Drosophila melanogaster*. *Genome Res.* 21:182–192.
- Hu H, Li X. 2007. Transcriptional regulation in eukaryotic ribosomal protein genes. *Genomics* 90:421–423.
- Kanamori-Katayama M, Itoh M, Kawaji H, et al. (13 co-authors). 2011. Unamplified cap analysis of gene expression on a single-molecule sequencer. *Genome Res.* 21:1150–1159.
- Kodzius R, Kojima M, Nishiyori H, et al. (12 co-authors). 2006. CAGE: cap analysis of gene expression. *Nat Methods.* 3:211–222.
- Li H, Durbin R. 2009. Fast and accurate short read alignment with Burrows-Wheeler transform. *Bioinformatics* 25:1754–1760.
- Malherbe Y, Kamping A, van Delden W, van de Zande L. 2005. ADH enzyme activity and Adh gene expression in *Drosophila melanogaster* lines differentially selected for increased alcohol tolerance. *J Evol Biol.* 18:811–819.
- Nickel W, Seedorf M. 2008. Unconventional mechanisms of protein transport to the cell surface of eukaryotic cells. *Annu Rev Cell Dev Biol.* 24:287–308.
- Ni T, Corcoran DL, Rach EA, Song S, Spana EP, Gao Y, Ohler U, Zhu J. 2010. A paired-end sequencing strategy to map the complex landscape of transcription initiation. *Nat Methods.* 7:521–527.
- Nolte V, Pandey RV, Kofler R, Schlötterer C. 2013. Genome-wide patterns of natural variation reveal strong selective sweeps and ongoing genomic conflict in *Drosophila mauritiana*. *Genome Res.* 23:99–110.
- Ogueta M, Cibik O, Eltrop R, Schneider A, Scholz H. 2010. The influence of Adh function on ethanol preference and tolerance in adult *Drosophila melanogaster*. *Chem Senses.* 35:813–822.
- Ohler U, Liao GC, Niemann H, Rubin GM. 2002. Computational analysis of core promoters in the *Drosophila* genome. *Genome Biol.* 3: RESEARCH0087.
- Ohno S. 1970. Evolution by gene duplication. London: George Allen & Unwin Ltd.
- Papacit M, Orengo D, Juan E. 2004. Sequences upstream of the homologous cis-elements of the Adh adult enhancer of *Drosophila* are required for maximal levels of Adh gene transcription in adults of *Scaptodrosophila lebanonensis*. *Genetics* 167: 289–299.
- Park C, Makova K. 2009. Coding region structural heterogeneity and turnover of transcription start sites contribute to divergence in expression between duplicate genes. *Genome Biol.* 10:R10.
- Plessy C, Bertin N, Takahashi H, et al. (24 co-authors). 2010. Linking promoters to functional transcripts in small samples with nanoCAGE and CAGEscan. *Nat Methods.* 7:528–534.
- Posakony JW, Fischer JA, Maniatis T. 1985. Identification of DNA sequences required for the regulation of *Drosophila* alcohol dehydrogenase gene expression. *Cold Spring Harbor Symp Quant Biol.* 50:515–520.
- Rach EA, Yuan HY, Majoros WH, Tomancak P, Ohler U. 2009. Motif composition, conservation and condition-specificity of single and alternative transcription start sites in the *Drosophila* genome. *Genome Biol.* 10:R73.
- Salimullah M, Sakai M, Mizuho S, Plessy C, Carninci P. 2011. NanoCAGE: a high-resolution technique to discover and interrogate cell transcriptomes. *Cold Spring Harb Protoc.* 2011: pdb.prot5559.
- Sandelin A, Carninci P, Lenhard B, Ponjavic J, Hayashizaki Y, Hume DA. 2007. Mammalian RNA polymerase II core promoters: insights from genome-wide studies. *Nat Rev Genet.* 8:424–436.
- Shin HD, Winkler C, Stephens JC, et al. (15 co-authors). 2000. Genetic restriction of HIV-1 pathogenesis to AIDS by promoter alleles of IL10. *Proc Natl Acad Sci U S A.* 97:14467–14472.
- Shiraki T, Kondo S, Katayama S, et al. (17 co-authors). 2003. Cap analysis gene expression for high-throughput analysis of transcriptional starting point and identification of promoter usage. *Proc Natl Acad Sci U S A.* 100:15776–15781.
- Sorourian M. 2010. Turnover and lineage-specific broadening of the transcription start site in a testis-specific retrogene. *Fly* 4:3–11.
- Suzuki Y, Yoshitomo-Nakagawa K, Maruyama K, Suyama A, Sugano S. 1997. Construction and characterization of a full length-enriched and a 5'-end-enriched cDNA library. *Gene* 200:149–156.
- Wittkopp PJ, Haerum BK, Clark AG. 2004. Evolutionary changes in cis and trans gene regulation. *Nature* 430:85–88.
- Wray GA. 2003. Transcriptional regulation and the evolution of development. *Int J Dev Biol.* 47:675–684.